Hindawi
Shock and Vibration
Volume 2022, Article ID 7317247, 14 pages
https://doi.org/10.1155/2022/7317247

Research Article

Key Technology Research on the Rapid-Molding In-Closed Retaining-Wall in Filling Mining

Chaowen Hu,[1,2,3] **Qian Li**,[2] **Yilong Wang**,[2] **Ke Chang**,[4] **Yongyuan Li**,[2] **Yaqian Wang**,[5] **and Hui Liu**[6]

[1]*China Huaneng Group Co., Ltd., Beijing 100031, China*
[2]*Huaneng Coal Technology Research Co., Ltd, ., Beijing 100070, China*
[3]*Transportation Institute, Inner Mongolia University, Hohhot, Inner Mongolia 010070, China*
[4]*Sihe Coal Mine, Jinneng Holiding Group Co., Ltd., Jincheng, Shanxi 048000, China*
[5]*Weifang Xiashan271 Experimental Middle School, Weifang, Shandong 261325, China*
[6]*Shenmu Ningtiaota Coal Mining Company Ltd., Shaanxi Coal Mining Group, Yulin 719300, China*

Correspondence should be addressed to Chaowen Hu; chaowen_hu@163.com

Received 3 November 2021; Revised 23 February 2022; Accepted 11 March 2022; Published 9 April 2022

Academic Editor: Xing Li

Filling mining is a main technology of mining coal resources under buildings, and it has a good effect on preventing ground subsidence. Taking Wangtaipu coal mine of the Shanxi Jincheng Anthracite Coal Mining Group as the engineering background, in order to solve the problem of traditional closed brick wall at the end of working face, which consumes a lot of manpower and material resources, and low efficiency, a technology of rapid-molding in-closed retaining-wall was proposed. Through theoretical analysis and engineering analogy, the overall structure and size of the mold bag were designed. Through the experiment of high-water bleeding rate and slurry expansion, it was determined that the best water-cement ratio was 0.85 : 1, and the best additive content was 25 kg/m^3. Taking economic factors into consideration, it was determined that liquid sodium silicate was used as the admixture. The XV2308 working face was selected for on-site testing and the on-site monitoring of the roof pressure, the roadway deformation, and the stress of the coal body. The results showed that there was no large area roof pressure on the working face, the coal body was under stable force, the stress concentration coefficient was small, the coal pillar had no plastic failure, and the roadway deformation was small. Through on-site monitoring of ground subsidence, the results showed that the amount of ground movement and deformation were small. The maximum value of subsidence was 12 mm, which could meet the requirements of safety production and had significant economic benefits.

1. Introduction

With the rapid development of China's infrastructure construction, coal resources under buildings become more and more common [1–4]. According to statistics, the total amount of coal resources under buildings in China is about 8.5 billion tons, which is a tremendous waste of coal resources [5–8]. At present, filling mining is an effective method to solve the problem of coal resources under buildings [9–11]. From the bottom to the top, filling mining can effectively control floor water inrush, rock fracture and migration, rock burst and mine pressure, and surface subsidence. In the process of filling mining practice, from the point of view of mine pressure and strata control, increasing the filling rate can effectively control strata movement and surface subsidence, while from the point of view of prevention and control of surface subsidence [12, 13]. With the development of material science, filling materials have gradually developed from solid wastes such as coal gangue in the early stage to paste materials, paste-like materials, high-water materials, and ultra-high-water materials [14–17]. However, due to the complex geological of coal mine, the filling cycle is long, and the filling process is complex. In order to improve the efficiency of construction

operation, reduce the filling preparation time, and relieve the tension between backfill and mining in continuous mining face, it is necessary to carry out improved experimental research on the sealing wall at the end of stope roadway. In this study, Wangtaipu coal mine is used as the engineering background to study the technology of rapid-molding in-closed retaining-wall in filling mining.

2. Engineering Background

Wangtaipu coal mine is a large-scale coal mine owned by the Shanxi Jincheng Anthracite Coal Mining Group. It was put into production as early as 1964. After more than 50 years of mining, Wangtaipu coal mine has very few mineable coal reserves, and most of them are under buildings. The number of coal reserves of #9 coal seam under buildings are about 19.753 million tons, and the number of coal reserves of #15 coal seam under buildings are about 37.707 million tons. The coal reserves of the two mineable coal seams under buildings are as high as 57 million tons.

Wangtaipu coal mine began a high-water material filling test in 2012. The traditional brick wall was used to construct a seal wall. A total of 42 vehicles of foamed cement bricks, red bricks, cement, sand, and stone powder were required to build the brick wall. It consumed a lot of material and labor, which brought great difficulties to underground transportation, and the efficiency of the enclosed brick wall was low, which seriously restricted the production efficiency of filling and mining. In order to ensure the mining speed of the working face and alleviate the contradiction between the process of mining and filling, the method of mold bag was proposed to improve the efficiency of the closed-end sealing filling.

This article chose the XV2308 working face of Wangtaipu coal mine as the engineering background. The mineable coal seam of the XV2308 working face was the #15 coal seam, the mining height was 2.5 m, the dip angle was 1°-2°. The direct roof stratum of XV2308 working face was K2 limestone with a thickness of 7.54–11.38 m, and the average was 9.32 m. The top of the direct roof stratum contained a layered flint strip. The uniaxial compressive strength was 53.6–212.9 MPa, and the average was 101.6 MPa. The uniaxial tensile stress was 2.2–6.1 MPa, and the average was 4.0 MPa, and the shear strength was 5.7–16.0 MPa, and the average was 13.2 MPa. The direct floor stratum was mudstone with an average thickness of 2.75 m, and its lower part was bauxite mudstone with an average thickness of 4.25 m. The uniaxial compressive strength was 12.1–58.4 MPa, and the average was 28.3 MPa; the uniaxial tensile strength was 0.7–2.0 MPa, and the average was 1.4 MPa; and the shear strength was 1.9–6.6 MPa, and the average was 4.2 MPa.

The continuous mining and filling working face mainly has two working links: mining and filling. After the stope roadway is excavated, the construction speed of the closed retaining walls at ends is too slow, which restricts the filling efficiency. Therefore, the technology of the rapid-molding in-closed retaining-wall is proposed. The design concept of the rapid-molding in-closed retaining-wall is derived from the technology of mold bag concrete cofferdam slope protection [18, 19]. The design idea of this technology is that use high-strength fireproof fiber cloth to sew into a mold bag, hang the mold bag on the roof of the stope roadway end, carry out side support treatment on the front and rear facades, and then pour high-water filling slurry into the mold bag. This study analyzes the size of the mold bag, optimizes the filling material, and identifies the suitable admixtures.

3. Design of a Closed Wall for Rapid Prototyping of Mold Bag in the End

3.1. Overall Structure of the Mold Bag. As shown in Figure 1, the shape of mold bag was cube, made of high-strength fire-retardant fiber cloth [16, 17]. Other structures included hanging bag sleeves that hang the mold bag on the roof stratum of the roadway; mold bag filling port which was used to fill the mold bag with filling materials; filling openings of the stope for filling and grouting; venting holes for exhausting; and strong rib holes of the mold bag used to penetrate the strong rib, which was used to limit the large deformation of the mold bag when the grout was poured.

3.2. Size of Mold Bag. The width of the mold bag should be able to ensure that the two sides of the mold bag can be in close contact with the coal wall and play an effective supporting role. The height of the mold bag should ensure that the mold bag can still be in contact with the floor stratum when it was hung on the roof stratum. The thickness of the mold bag should be able to ensure that the mold bag can be formed on its own after filling with the filling material and can effectively offset the lateral pressure of the stope roadway during slurry filling.

The size of the mold bag needs to consider the section size of roadway, the row spacing between bolts, and the construction conditions on-site. The width of the mold bag also needs to consider the peripheral length of the roadway and the amount reserved. Considering the error of the roadway and the soft coal side, the width allowance of the mold bag was designed to be 300–500 mm, and the height allowance was designed to be 100 mm. The schematic of the mold bag of the 9 m section is shown in Figure 2.

4. Performance Optimization of High-Water-Based Filling Material and the Experimental Study of Admixture

4.1. The Curing Mechanism of High-Water Materials. The curing process of high-water materials is mainly divided into three stages: hydration period, hydraulic period, and strength period [18–20]. The chemical reaction formula of each stage is as follows: $3CaO{\cdot}SiO_2 + nH_2O = xCaO{\cdot}SiO_2{\cdot}yH_2O + (3\text{-}x)\ Ca\ (OH)_2$, $2\ (2CaO{\cdot}SiO_2) + 4H_2O = 3CaO{\cdot}2SiO_2{\cdot}3H_2O + Ca\ (OH)_2$, $3CaO{\cdot}Al_2O_3 + 6H_2O = 3CaO{\cdot}Al_2O_3{\cdot}6H_2O$.

As shown in Figure 3, a given mass of flocculent structure has been formed in the fly ash filling body at the age of 3 days. When the age of 7 days is reached, the flocculent structure increases significantly and overlaps each other closely, and then, the filling body has a certain strength.

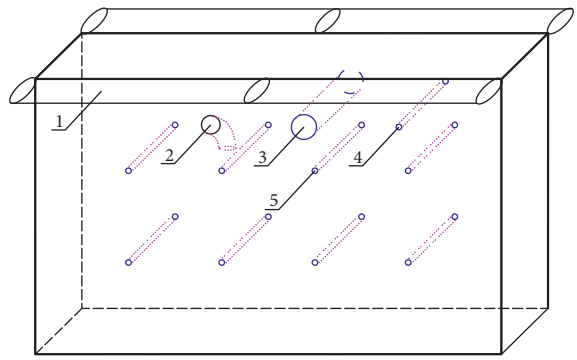

Figure 1: Schematic diagram of mold bag.

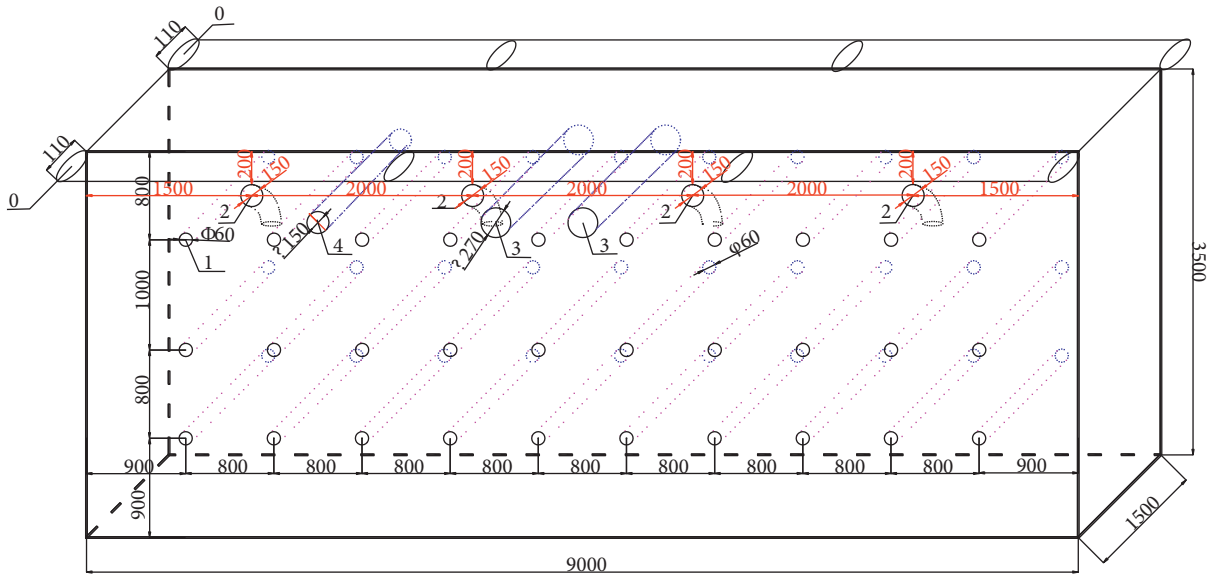

Figure 2: Schematic of the mold bag of the 9 m section.

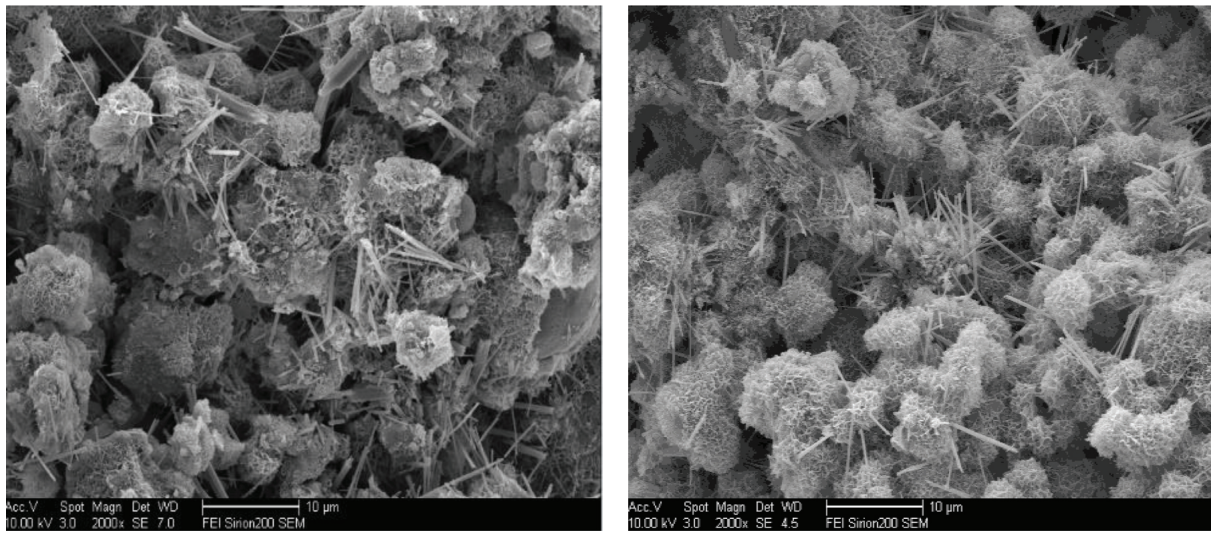

(a) (b)

Figure 3: Scanning electron micrograph of fly ash filling body with (a) 3 days and (b) 5 days.

4.2. Optimization and Performance Improvement of High-Water Filling Materials. At the beginning of the test, the water-solid mass ratio of the filling material was 0.7 : 1, and the early strength of the filling material was low. The average strength of 14-day was 2.19 MPa and the 28-day was 3.42 MPa. The strength of the filling material could not meet the requirements of the production demand. The problems were also manifested in two aspects: the high bleeding rate and the shrinkage of the filling body. The change of the slurry bleeding rate and the expansion rate at the beginning of the test is shown in Figure 4.

As shown in Figure 4, the bleeding rate of the slurry was large, the maximum value was 24.6% at the #2 measuring point, the minimum was 2.36% at the #6 measuring point, and the average was 11.8%; the bleeding rate of the measurement points in the roadway of each stope was quite different, the properties of filling material was affected by the material formula, technology, and other factors, and the bleeding performance was not controlled; except for the bleeding rate of #6 measuring point was less than 3%, the other measuring points were more than 3%, and the excess amount was large; after the filling material solidifies, there was almost no expansion. Except for the expansion rate of the roadway in #1 stope was 2.58%, the filling body in other parts had the phenomenon of dry shrinkage, the maximum value of shrinkage was 8.0%, and the average was 3.47%; the dry shrinkage of the filling body was stable in the early stage, with an average of 2.58%. In the later stage, due to the improvement of the material formulation, the slurry was unstable, and the dry shrinkage increased to 6.64% on average.

Aiming at the problem of bleeding rate and expansion rate of the filling material, the additive content and the water-cement ratio of the filling material were adjusted. The additive increased from 5 kg/m^3 to 25 kg/m^3. The water-cement ratio decreased from 1 : 1 to 0.85 : 1. The change of the bleeding rate of the improved filling material is shown in Figure 5(a), and the change of the expansion rate of the improved filling material is shown in Figure 5(b).

As shown in Figure 5, the bleeding rate of the filling material decreased from 5.8% to 0; the monitoring results in mid-February showed that the bleeding rate of the filling material was 3.0% on average, the monitoring results from June to September showed that the bleeding rate of the filling material was 0.28% on average, and the bleeding rate of the filling material was effective to control; the expansion rate of the filling material was all positive values, which means that the solidified filling body will not dry shrinkage and will expand to a certain extent; the monitoring results in mid-February showed that the expansion rate of the filling material was 4% on average. The monitoring results from June to September showed that the minimum value of the expansion rate of the filling material was 5%, and the average was 10%.

By comparing and analyzing the properties of the filling material in the early stage and after the improvement, it can be seen that the improved filling material was better than the previous material in bleeding rate and expansion rate, so that can be directly filled and connected to the roof, which ensured the effect of controlling the roof; in terms of the expansion rate, the initial filling material had a certain dry shrinkage, with an average dry shrinkage rate of 3.47%. The volume expansion rate of the improved material was above 5%, which was more conducive to filling and topping; in terms of the bleeding rate, the average bleeding rate of initial filling material was 11.8%. After improvement, the bleeding rate of the filling material was reduced to 0.28%, which made the stope roadway easier to fill and connect to the roof.

4.3. Admixture Experiment

4.3.1. Introduction to the Experiment. The experiment was based on the design ratio of the high-water filling material to prepare the mixed slurry, then added the admixture and stirred evenly, poured the mixed slurry into the standard test mold, and put it into the curing box [21, 22]. The curing conditions were set at 42°C and 95% humidity.

4.3.2. Experiment Process

(1) Prepared slurry. After the slurry was prepared, poured it into the standard test mold for curing. According to the volume of a single trial mold, needed to prepare 1000 ml slurry and selected an electronic scale with a range of 1.0 kg and an accuracy of 0.1 g to weigh the material. According to the proportion of the filling slurry, weighed the ingredients in equal proportions, poured them into a mixing tank, added water and mix, stirred for no less than 5 minutes, added additives, and stirred for 1 minute until the slurry was uniform.

(2) Made a trial model. Assembled the standard test mold, sealed the gap with wax, and then poured the slurry into it.

(3) Maintenance. Put the test model into the curing box for curing, adjusted the curing temperature to 40°C according to the measured reaction temperature of the slurry in the well, and adjusted the humidity to 95% according to the curing humidity condition in the hydraulic concrete test procedure.

4.3.3. Result. According to the above analysis, separate and combined tests were carried out on different admixtures, and the results are given in Table 1.

Each group of reagents had three groups of additive amounts, each group of tests was not less than 3 times, and the test took the best result as the final result.

According to the material characteristics of the mold bag, the shorter the time required for the filling material to solidify after being poured, the better it was to improve the sealing effect, topping effect, and production efficiency. Therefore, the test results of the 5th and 6th experiments met the requirements. Considering the factors of production cost, the price of industrial liquid sodium silicate was much lower than industrial alum, and it was more convenient to use liquid sodium silicate as an admixture [23–25].

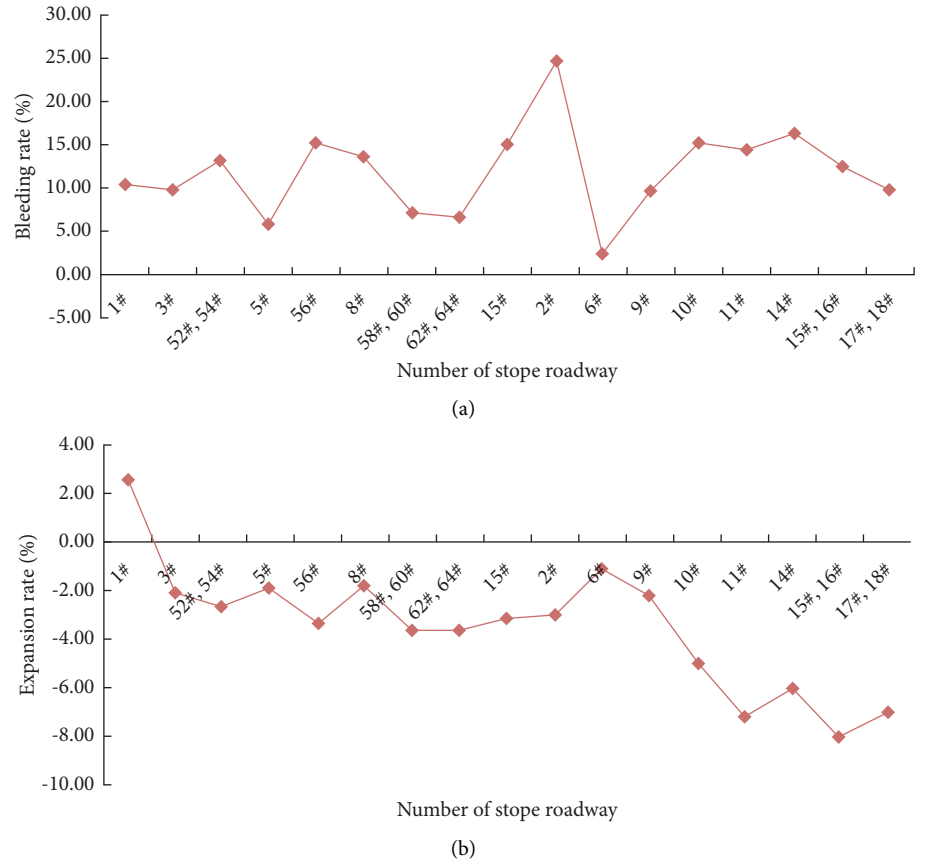

Figure 4: Experimental monitoring curve of (a) slurry bleeding rate and (b) expansion rate.

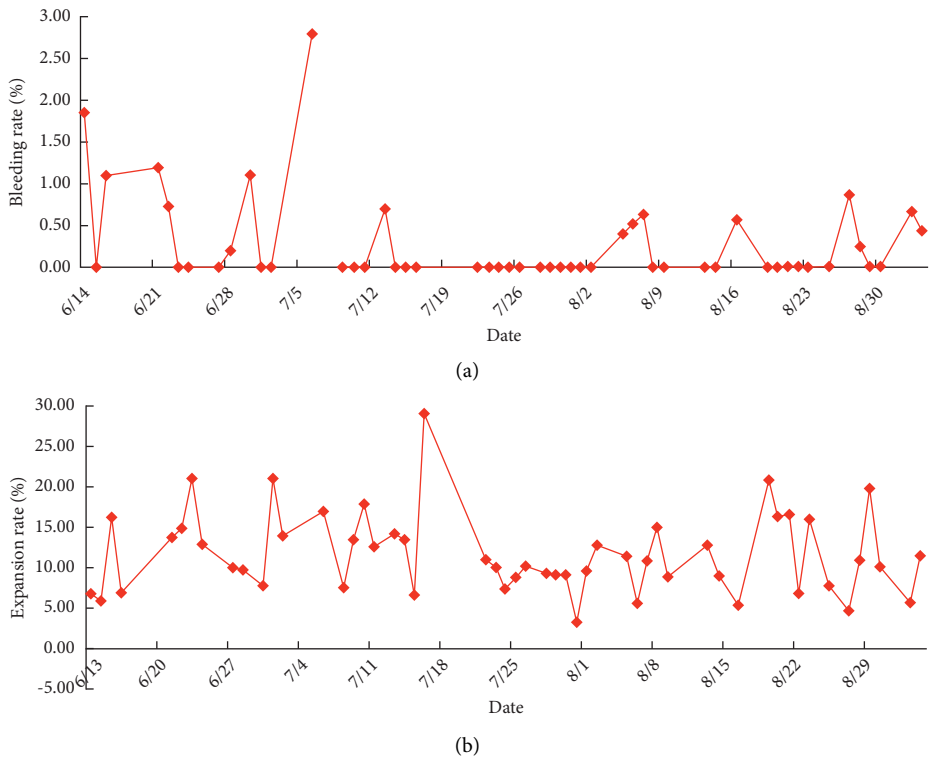

Figure 5: Improved filling material test curve of (a) bleeding rate and (b) expansion rate.

Table 1: Admixture test results.

No.	Admixture	Test result		
		30 min	3 h	12 h or more
1	Calcium chloride	Noninitial set	Noninitial set	Initial set, nonstrength, bleeding, nonexpanded
2	Bentonite	Noninitial set	Noninitial set	Initial set, nonstrength, bleeding, nonexpanded
3	Bentonite, urea	Initial set	Nonfinal set	Final set, intensity contrast, bleeding, poor expansion
4	Calcium sulphoaluminate, sodium sulfate	Noninitial set	Initial set	Final set, low strength, bleeding, nonexpanded
5	Liquid sodium silicate	Initial set	Final set	Final set, medium strength, nonbleeding, microdilatancy
6	Alum, liquid sodium silicate	Initial set	Final set	Final set, great strength, nonbleeding, microdilatancy

Therefore, liquid sodium silicate was finally selected as an admixture for the filling material of the mold bag.

The modulus of silica and alkali metal oxides in water glass is called the modulus [26–28], and the alkalinity of water glass is inversely proportional to its modulus value. When the modulus is constant, the greater the concentration of water glass, the greater its density and the stronger the bonding force. When the modulus value is small, although its early strength is high, its late strength is low. According to the test results, the reasonable modulus of water glass was 2.0, in the high-water filling slurry with a mass ratio of 5%, which can ensure that the filling slurry initially set within 3 minutes, finally set within 3 hours, the uniaxial compressive strength reached 0.8 MPa within 5 hours, and met the pressure requirements of closed walls.

5. Field Test

5.1. Overview of the Test Site. According to the filling and mining progress of the XV2308 working face, it was designed to conduct field tests in the roadway in 10th stope, 18th stope, 26th stope, and 50th stope. The test sites are shown in Figure 6.

The roof stratum of the XV2308 working face was limestone, which was dense, hard, and flat; the floor stratum was mudstone, which was easy to soften in contact with water. Therefore, the cutting depth was not less than 300 mm to ensure the sealing effect of the mold bag retaining wall. The two ribs were cut by a continuous mining machine, which was flat, and the cutting depth was 150–200 mm. The roof and two ribs are shown in Figure 7; the mold bag hung on the roof stratum of the roadway end in the filling stop is shown in Figure 8; the filling process of the mold bag is shown in Figure 9; the effect of the filling body in the mold bag after solidification is shown in Figure 10.

5.2. On-Site Monitoring

5.2.1. Monitoring of the Mine Pressure. Given the mining and support of the XV2308 working face, the monitoring contents were determined as roof pressure, roadway surrounding rock deformation, and coal stress [29, 30]. The XV2308 working face was filled with high-water materials. Due to the high-water materials had good fluidity, water in the materials was easy to seep into the monitoring equipment. Therefore, special monitoring roadways were designed with mine pressure monitoring equipment. In order to research the changes in the stress of the coal body and the stress and deformation of the filling body in the process of filling mining, it was planned to design two special monitoring roadways to install monitoring equipment. The two monitoring roadways were recorded as #27 monitoring roadway and #34 monitoring roadway, respectively. The size of the roadways were width × height = 6.0 × 2.5 m, with a coal pillar of 6.0 m on each side, and the two monitoring roadways were not filled. The layout of the monitoring stations is shown in Figure 11.

5.2.2. Online Monitoring of Roof Pressure. The force of bolts and anchor cables was monitored, and the pressure characteristics during the process of filling mining were analyzed through the field monitoring data. Arrange bolt and anchor cable dynamometers are in the centralized haulage roadway, XV2215 centralized roadway, XV2216 centralized roadway, ventilation roadway, #27 roadway, and #34 monitoring roadway, respectively.

5.2.3. Monitoring of Bolt Force. Considering the characteristics of the continuous coal mining machine, the installation distance of the bolt dynamometer measuring stations in the haulage roadway was designed to be 30 m and a total of 7 measuring stations. In order to research the change in roof pressure of working face in tendency, the installation spacing of the bolt dynamometer stations in the roadways of #27 and #34 monitoring stopes was 20 m, and 5 measuring stations were installed in each stope roadway, a total of 10 stations. The installation spacing of the bolt dynamometer stations in the ventilation roadway was 30 m and a total of 7 stations. The installation spacing of bolt dynamometer measuring stations was 40 m in XV2215 and XV2216 centralized roadway, XV2215 centralized roadway was arranged with 5 measuring stations, and XV2216 centralized roadway was arranged with 4 measuring stations, a total of 9 measuring stations. A total of 33 bolt force monitoring points were arranged. The measuring points of the concentrated roadway and the ventilation roadway were arranged in an E type. There were also measuring points arranged in the mine pressure monitoring roadway, which can carry out a comprehensive roof pressure monitoring on the working face and analyze the pressure change characteristics and laws of the direction and tendency of the roof during the entire filling and mining process.

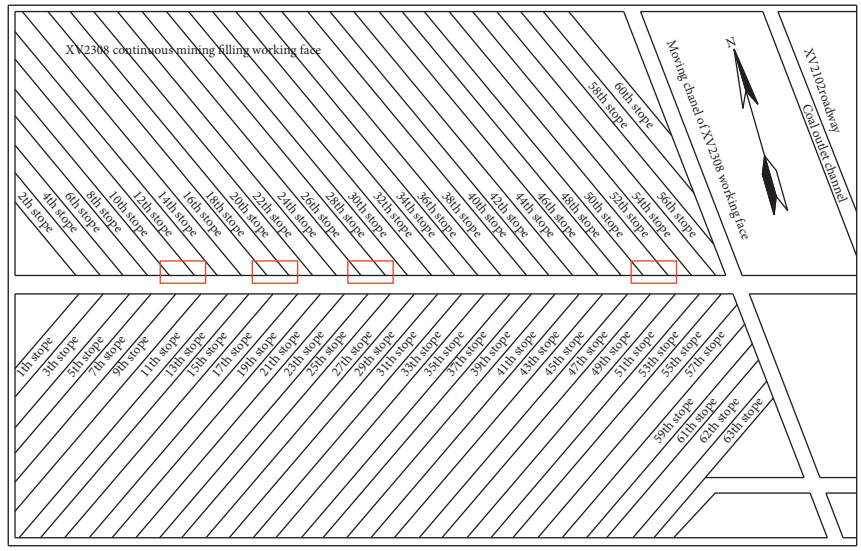

Figure 6: The test sites.

(a) (b) (c)

Figure 7: The state of (a) left rib, (b) right rib, and (c) roof.

Figure 8: The mold bag hung on the roof.

Figure 9: Mold bag filling completed.

5.2.4. Monitoring of Anchor Cable Force. According to the characteristics of continuous coal mining machine, the installation distance of the anchor cable dynamometer measuring station in the centralized haulage roadway was 60 m, a total of 3 measuring stations. The installation spacing of anchor cable dynamometer stations in the roadways of #27 and #34 stopes was 40 m, and 2 measuring stations were installed in each roadway, a total of 4 measuring stations. The installation distance of the anchor cable dynamometer measuring station was 40 m in the ventilation roadway, a total of 5 measuring stations. The installation spacing of the anchor cable dynamometer stations in the XV2215 and XV2216 concentrated roadways was 70 m, and 2 measuring

Figure 10: The effect of the filling body in the mold bag after solidification.

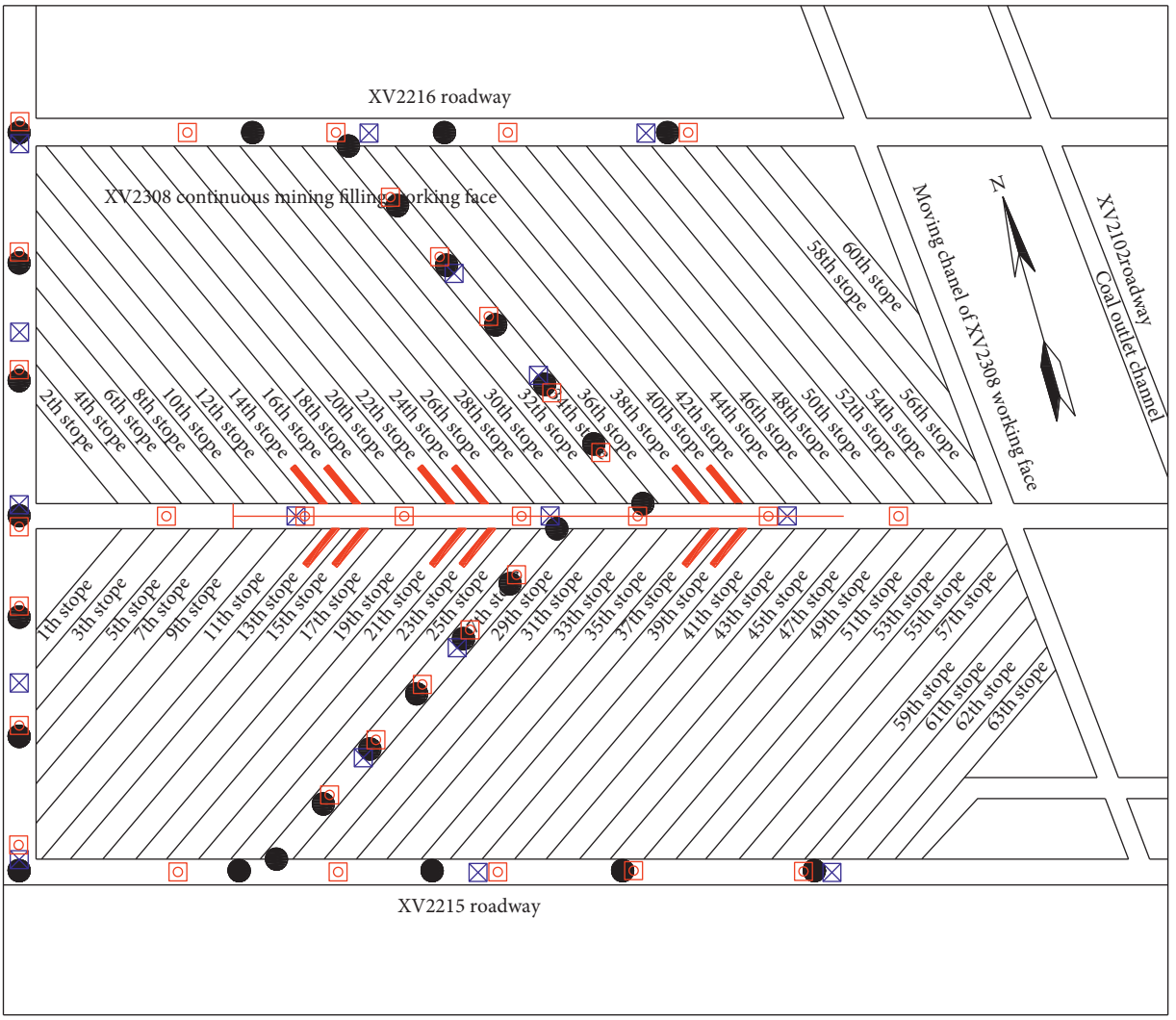

Figure 11: The layout of the monitoring stations.

stations were installed in each roadway, a total of 4 measuring stations. A total of 16 measuring stations were arranged.

The force of bolt (anchor) was monitored on-site for the XV2308 concentrated roadway, XV2308 ventilation roadway, XV2215 roadway, XV2216 roadway, #27 stope roadway, and #34 stope, respectively. The monitoring curves are shown in Figure 12.

As shown in Figure 12, except for the 34th stope measuring station and the XV2216-120 m bolt measuring station, the overall change in the face of bolt and anchor cable was small.

(i) In the mining process of the working face, except for the large changes in the partial area, the overall force change was small, indicating that filling mining prevents the direct roof from moving and breaking, reducing the force of the bolt (anchor), and made the force more uniform.

(ii) It can be seen from the monitoring curves of the #34 stope roadway that its change rule was different from other roadway measuring stations, which indicated that the roof of the roadway in this stope was broken, and the direct roof had moved and deformed.

(iii) When mining #42 and #43 stopes, the force of bolt (anchor) in the positions of 100 m increased rapidly, indicating that the mining near the roadway would cause the displacement of the broken roof, and the supporting effect of the bolt (anchor) could limit the displacement; then, the force of the bolt (anchor) drops rapidly to the value before the change and remained unchanged.

(iv) Overall, the bolt (anchor) of the working face was relatively stable in force, the mining pressure was small, and there was no large area roof pressure.

6. Monitoring of Roadway Deformation

In order to comprehensively analyze the change of the roof subsidence, the approaching amount of the roof and the floor, and the approaching amount of the two ribs of the roadway, there were, equipped with a roadway surface displacement measuring station in the centralized haulage roadway, the 27th stope roadway, the 34th stope roadway, the XV2215 centralized roadway, the XV2216 centralized roadway, and the ventilation roadway. The location of the measuring stations was the same as that of the bolt dynamometers. There were 7 measuring stations in the centralized haulage roadway, 5 measuring stations in each of the #27 and #34 stope, 7 measuring stations in the ventilation roadway, 5 measuring stations in the XV2215 centralized roadway, and 4 measuring stations in the XV2216 centralized roadway, a total of 33 measuring stations. The monitoring curves of the surface displacement are shown in Figure 13.

As shown in Figure 13, the following points are observed.

(1) The measurement points of #27 stope and #34 stope both showed a certain degree of surface displacement, and the change of #34 stope was more obvious than that of #27 stope. A total of 7 measuring points on the two survey lines had ribs approaching and roof sinking, and the maximum value of approaching distance was 35 mm, and the maximum value of sinking was 30 mm. There were 8 measuring points that had bottom drum; the maximum value of bottom drum was 60 mm, and the maximum deformation was at the 5# measuring point in the #34 stope.

(2) There was a certain degree of roof subsidence in the stope roadway. The maximum value of roof subsidence was 30 mm. This was related to the emptying time of the stope roadway. Therefore, the filling should be organized as soon as possible to ensure the control effect of the surface settlement.

(3) The approaching amount of the two ribs in the roadway was small, indicating that the filling mining could control the ground pressure of the working face, and the coal pillar had not undergone plastic failure and could ensure the stability of the coal pillar.

(4) A certain degree of bottom heave occurred in the roadway. The maximum value of bottom heave was 60 mm. This is because the bottom plate was made of bauxite mudstone, which becomes soft and swells in contact with water, resulting in bottom heave.

(5) In summary, the surface displacement of the stope roadway was small, which did not affect the use of the roadway.

7. Monitoring the Coal Body Stress

In order to research the distribution law of the advanced pressure of the roof and the change on the stress of the coal pillar during the filling mining process, the stress of the coal body was monitored. Two measuring stations in the XV2308 roadway were arranged, and each measuring station had six borehole stress gauges. The borehole stress gauges were installed at a depth of 9 m in the coal wall. There was a total of 12 borehole stress gauges in the two measuring stations. The monitoring curves of coal stress are shown in Figure 14.

As shown in Figure 14, the following points are observed.

(1) The force of the borehole stress gauge gradually increased with the mining of the working face, and the increment was about 3.5 MPa, indicating that the coal pillar receives less concentrated stress during the mining, which was beneficial to the control of the roof strata.

(2) During mining, the remaining coal pillars did not appear to be slicing, which was conducive to controlling the movement of the roof strata and surrounding rock and did not affect the quality of the coal mined in the subsequent stages.

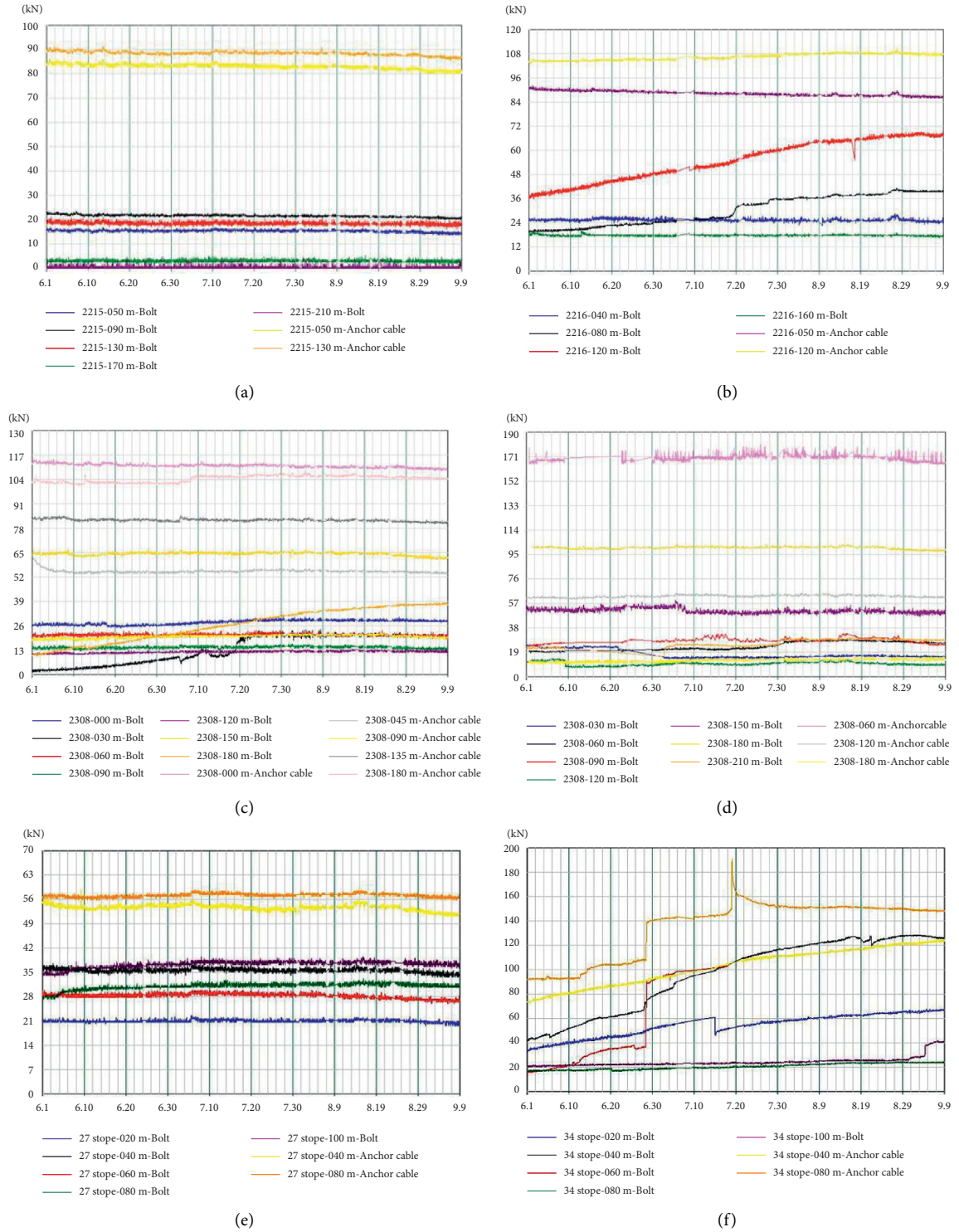

Figure 12: Force of bolt and anchor cable monitoring curves in the (a) XV2215 roadway, (b) XV2216 roadway, (c) XV2308 ventilation roadway, (d) XV2308 concentrated roadway, (e) #27 stope roadway, and (f) #34 stope roadway.

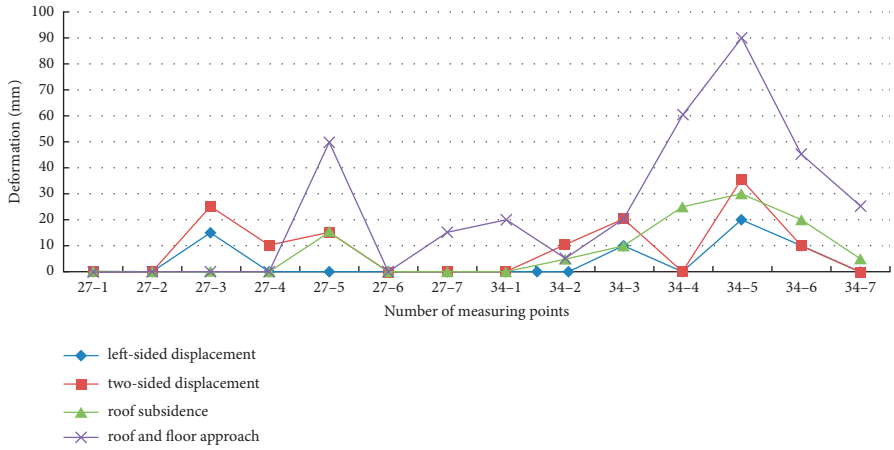

Figure 13: Monitoring curves of the surface displacement.

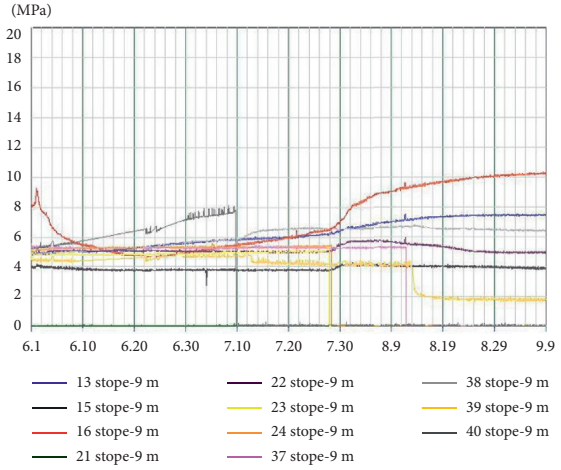

Figure 14: Monitoring curves of coal stress.

(3) In general, the coal body of the working face was under stable stress, the stress concentration coefficient was small, and there was no plastic failure in the coal pillar.

7.1. Observation and Research on Subsidence of the Ground Surface. The surface elevation corresponding to the XV2308 working face of Wangtaipu coal mine was 827–873 m. According to the mining situation and considering the actual topographical conditions, the observation station had a total of two survey lines, namely, the whole basin trend line D and the whole basin strike line C. The total length of the survey line was 1286 m, and 56 survey points were arranged. The layout of the stations is shown in Figure 15.

The monitoring curves of surface displacement monitored by the strike line are shown in Figure 16(a). The monitoring curves of surface displacement monitored by the trend line are shown in Figure 16(b). According to the monitoring data, the maximum value of subsidence of the ground surface was 12 mm, and the movement and deformation of the ground surface were small, which met the requirements of surface buildings.

After the field test in Wangtaipu coal mine, the technology of rapid-molding in-closed retaining-wall has a good application effect, and it is an effective method for mining coal resources under buildings. However, in the field test, it was also found that the mold bag has a poor application effect on special geological conditions such as broken surrounding rocks, geological structural belts, and large dip angles.

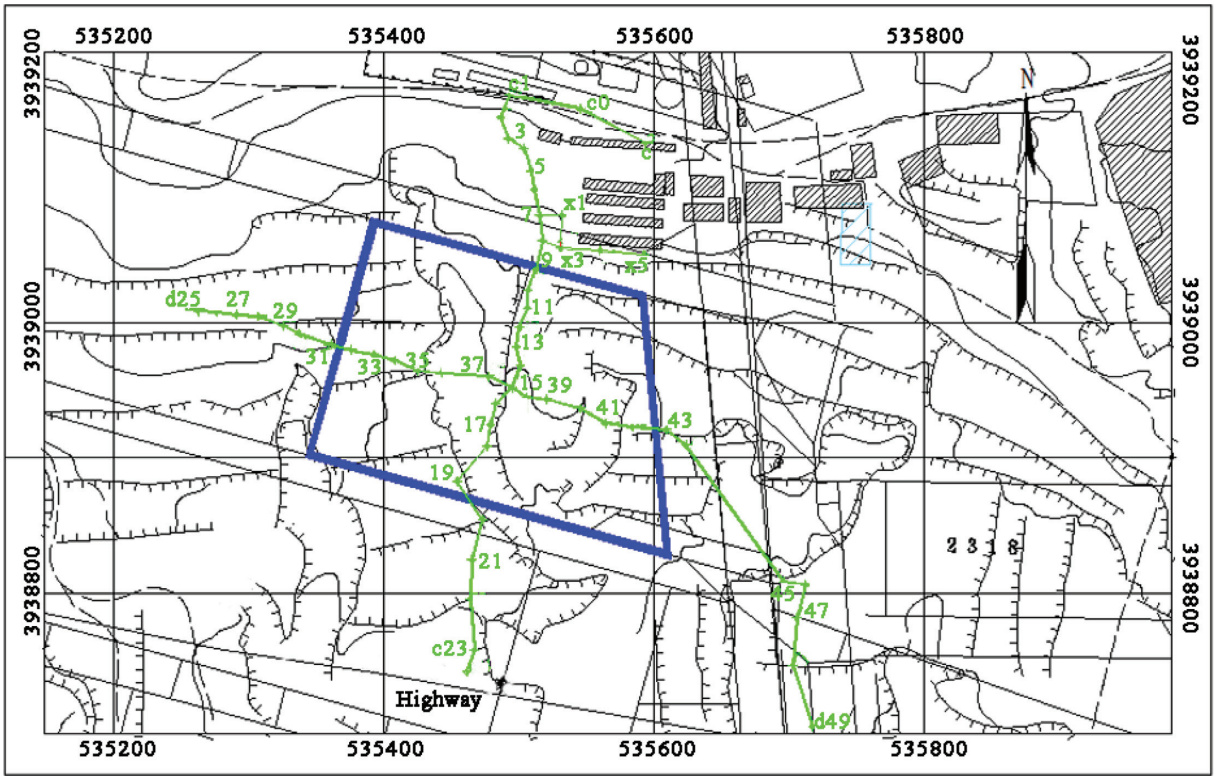

Figure 15: Layout of the stations.

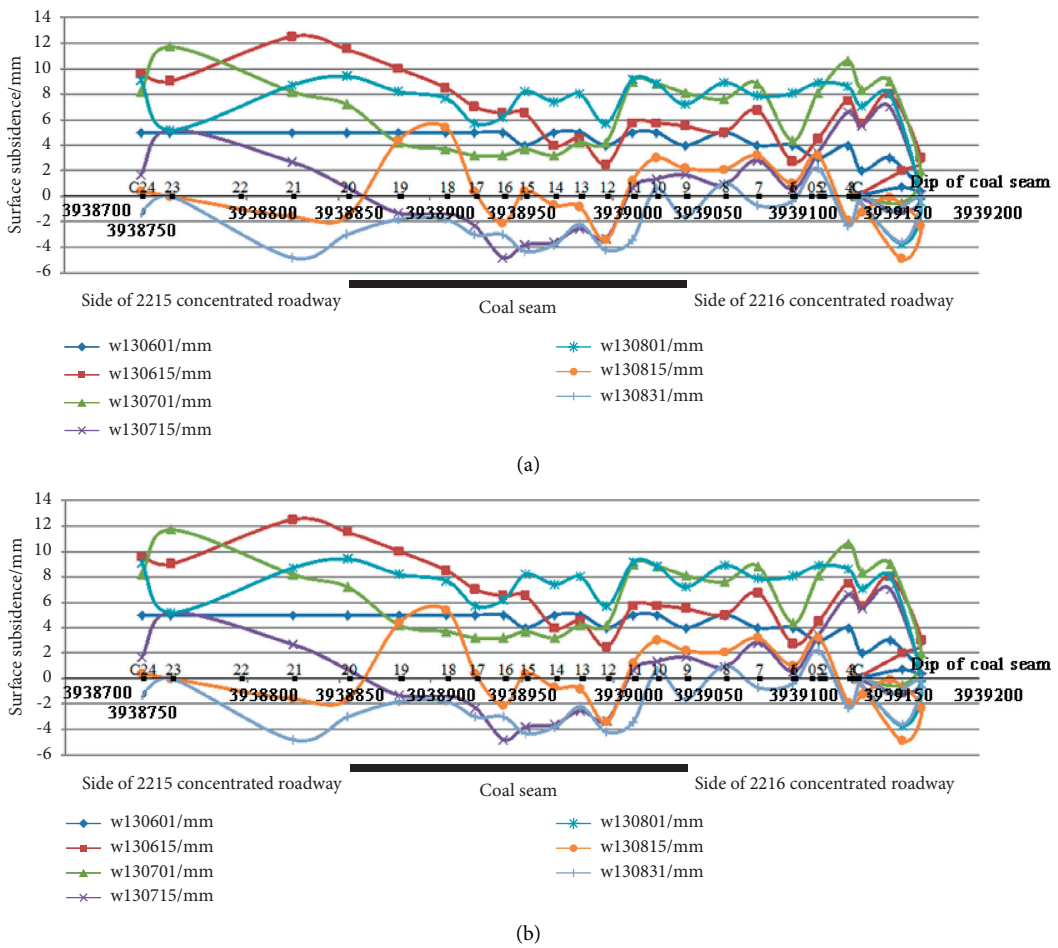

Figure 16: Monitoring curves of (a) the strike survey line and (b) the trend line.

8. Conclusions

In this study, through theoretical analysis, field monitoring, and industrial testing, the technology of rapid-molding inclosed retaining-wall in filling mining was studied, and the following conclusions were obtained.

(1) According to the coal seam occurrence in Wangtaipu coal mine, the structure and size of the mold bag were designed

(2) Through the test of bleeding rate of high-water material and swelling rate of slurry, it was determined that the best water-cement ratio was 0.85 : 1, and the best additive content was 25 kg/m^3.

(3) Through the admixture test and comprehensive consideration of economic factors, it was determined that liquid sodium silicate was the admixture for the filling material of the mold bag

(4) Through industrial tests, the results showed that the mold bag is small in size, light in weight, and convenient for underground transportation, which can reduce the transportation volume by more than 95% compared with the closed wall of brick-concrete structure. During the filling process, the mold bag does not rupture or collapse, and the construction is simple, convenient, and efficient. The construction speed is increased by more than 2 shifts, which improves the efficiency of continuous mining and filling and greatly reduces the labor intensity of workers. The comprehensive cost is reduced by more than 33%, and the economic benefits are significant.

Data Availability

The data used to support the findings of this study are available from the corresponding author upon request.

Conflicts of Interest

The authors declare that they have no conflicts of interest.

Authors' Contributions

All authors contributed to this study. Chaowen Hu and Qian Li conceptualized the study. Ke Chang and Yaqian Wang performed data curation. Yilong Wang performed formal analysis. Yongyuan Li and Hui Liu investigated the study. Chaowen Hu developed software. Qian Li developed methodology.

Acknowledgments

This work was supported by the higher educational scientific research projects of Inner Mongolia Autonomous Region (NJZY21291) and the Science and Technology Project of China Huaneng Group Co. Ltd. (HNKJ21-HF07).

References

[1] H. Z. Li, J. F. Zha, G. L. Guo, B. C. Zhao, and B. Wang, "Compression ratio design and research on lower coal seams in solid backfilling mining under urban areas," *Soil Mechanics and Foundation Engineering*, vol. 53, no. 2, pp. 125–131, 2016.

[2] L. Ma, Z. Jin, W. Liu, D. Zhang, and Y. Zhang, "Wongawilli roadway backfilling coal mining method - a case study in Wangtaipu coal mine," *International Journal of Oil, Gas and Coal Technology*, vol. 20, no. 3, pp. 342–359, 2019.

[3] S. Qiang, Z. Nan, W. J. Song, and Z. Xu, "Risk assessment and prevention of surface subsidence under buildings by cemented paste filling and strip mining methods: a Case Study," *Advances in Civil Engineering*, vol. 2021, Article ID 9965279, 10 pages, 2021.

[4] S.-j. Chen, F. Feng, Y.-j. Wang et al., "Tunnel failure in hard rock with multiple weak planes due to excavation unloading of in-situ stress," *Journal of Central South University*, vol. 27, no. 10, pp. 2864–2882, 2020.

[5] F. Feng, S. J. Chen, Y. J. Wang, W. P. Huang, and Z. Y. Han, "Cracking mechanism and strength criteria evaluation of granite affected by intermediate principal stresses subjected to unloading stress state," *International Journal of Rock Mechanics and Mining Sciences*, vol. 143, Article ID 104783, 17 pages, 2021.

[6] E. H. Bai, W. B. Guo, Y. Tan, G. S. Huang, M. J. Guo, and Z. B. Ma, "Roadway backfill mining with super-high-water material to protect surface buildings: a case study," *Applied Sciences-Basel*, vol. 10, no. 1, 12 pages, Article ID 10010107, 2019.

[7] H. Z. Li, G. L. Guo, and S. C. Zhai, "Mining scheme design for super-high water backfill strip mining under buildings: a Chinese case study," *Environmental Earth Sciences*, vol. 75, no. 12, 12 pages, Article ID 12665-016-5837-5, 2016.

[8] X. Liu, G. Guo, and H. Li, "Study on damage of shallow foundation building caused by surface curvature deformation in coal mining area," *KSCE Journal of Civil Engineering*, vol. 23, no. 11, pp. 4601–4610, 2019.

[9] J. Zhang, Q. Zhang, Q. Sun, R. Gao, D. Germain, and S. Abro, "Surface subsidence control theory and application to backfill coal mining technology," *Environmental Earth Sciences*, vol. 74, no. 2, pp. 1439–1448, 2015.

[10] F. Feng, X. B. Li, J. Rostami, D. X. Peng, D. Y. Li, and K. Du, "Numerical investigation of hard rock strength and fracturing under polyaxial compression based on Mogi-Coulomb failure criterion," *International Journal of Geomechanics*, vol. 19, no. 4, Article ID 04019005, 2019.

[11] D. Xuan and J. Xu, "Grout injection into bed separation to control surface subsidence during longwall mining under villages: case study of Liudian coal mine, China," *Natural Hazards*, vol. 73, no. 2, pp. 883–906, 2014.

[12] N. Jiang, C. Wang, H. Pan, D. Yin, and J. Ma, "Modeling study on the influence of the strip filling mining sequence on mining-induced failure," *Energy Science & Engineering*, vol. 8, no. 6, pp. 2239–2255, 2020.

[13] J. W. Liu, W. H. Sui, and Q. J. Zhao, "Environmentally sustainable mining: a case study of intermittent cut-and-fill mining under sand aquifers," *Environmental Earth Sciences*, vol. 7616 pages, 2017.

[14] C. X. Wang, Y. Liu, H. Hu, Y. Y. Li, and Y. Lu, "Study on filling material ratio and filling effect: taking coarse fly ash and coal gangue as the main filling component," *Advances in Civil Engineering*, vol. 2019, Article ID 2898019, 12 pages, 2019.

[15] H. Wang, J. Jiao, Y. M. Wang, and W. S. Du, "Feasibility of using gangue and fly ash as filling slurry materials," *Processes*, vol. 6, no. 12, 18 pages, Article ID 6120232, 2018.
[16] K. W. Rong, W. T. Lan, and H. Y. Li, "Industrial experiment of goaf filling using the filling materials based on hemihydrate phosphogypsum," *Minerals*, vol. 10, no. 4, 16 pages, Article ID 10040324, 2020.
[17] H. J. Luan, Y. J. Jiang, H. L. Lin, and Y. H. Wang, "A new thin seam backfill mining technology and its application," *Energies*, vol. 10, no. 12, 16 pages, Article ID 10122023, 2017.
[18] Z. Zheng, R. Liu, S. Li, and Q. Zhang, "Numerical modeling and verification of grouting with mold bag treatment on seepage failure in foundation excavation," *Geomatics, Natural Hazards and Risk*, vol. 9, no. 1, pp. 1172–1185, 2018.
[19] F. Yu, Z. K. Lou, and N. X. Yan, "Effect of the compounding of an antifoaming agent and a viscosity modifying agent on the frost resistance of mold bag concrete," *CONSTR BUILD MATER*, vol. 9, 2021.
[20] S. Wang, "Cofired biomass fly ashes in mortar: reduction of Alkali Silica Reaction (ASR) expansion, pore solution chemistry and the effects on compressive strength," *Construction and Building Materials*, vol. 82, pp. 123–132, 2015.
[21] R. Dhawan, B. M. S. Bisht, R. Kumar, S. Kumari, and S. K. Dhawan, "Recycling of plastic waste into tiles with reduced flammability and improved tensile strength," *Process Safety and Environmental Protection*, vol. 124, pp. 299–307, 2019.
[22] T. Li, G. B. Chen, Z. C. Qin, Q. H. Li, B. Cao, and Y. L. Liu, "The gob-side entry retaining with the high-water filling material in Xin'an Coal Mine," *Geomechanics and Engineering*, vol. 22, no. 6, pp. 541–552, 2020.
[23] X. Wang, D. Zhang, C. Sun, and Y. Wang, "Surface subsidence control during bag filling mining of super high-water content material in the Handan mining area," *International Journal of Oil, Gas and Coal Technology*, vol. 13, no. 1, pp. 87–102, 2016.
[24] X. L. Li and C. W. Liu, "Mechanical properties and damage constitutive model of high water material at different loading rates," *Advanced Engineering Materials*, vol. 20, no. 6, 15 pages, Article ID 201701098, 2018.
[25] V. Vasugi and K. Ramamurthy, "Identification of admixture for pelletization and strength enhancement of sintered coal pond ash aggregate through statistically designed experiments," *Materials & Design*, vol. 60, pp. 563–575, 2014.
[26] Z. T. Ahmed, D. W. Hand, M. K. Watkins, and L. L. Sutter, "Air-entraining admixture partitioning and adsorption by fly ash in concrete," *Industrial & Engineering Chemistry Research*, vol. 53, no. 11, pp. 4239–4246, 2014.
[27] L. Jin, G. D. Huang, Y. Y. Li, X. Y. Zhang, Y. S. Ji, and Z. S. Xu, "Positive influence of liquid sodium silicate on the setting time, polymerization, and strength development mechanism of MSWI bottom ash alkali-activated mortars," *Materials*, vol. 14, no. 8, 17 pages, Article ID 14081927, 2021.
[28] G. D. Huang, Y. S. Ji, J. Li, L. L. Zhang, X. Y. Liu, and B. L. Liu, "Effect of activated silica on polymerization mechanism and strength development of MSWI bottom ash alkali-activated mortars," *Construction and Building Materials*, vol. 201, pp. 90–99, 2020.
[29] F. Noritake and K. Kawamura, "Structural transformations in sodium silicate liquids under pressure: a molecular dynamics study," *Journal of Non-crystalline Solids*, vol. 447, pp. 141–149, 2016.
[30] R. A. Shishkin, N. A. Erkhova, A. R. Beketov, and A. A. Elagin, "Water-glass-based thermal paste for high-temperature applications," *Journal of Ceramic Science and Technology*, vol. 5, no. 3, pp. 199–202, 2014.